Adaptive Removal of the Transcranial Alternating Current Stimulation Artifact from the Electroencephalogram

Robert Guggenberger[1,*] and N.N.[1]

[1]Department for Translational Neurosurgery, University Hospital Tübingen
[*]Corresponding author: robert.guggenberger@posteo.eu

April 24, 2017

Abstract

Your abstract.

1 Introduction

The combination of transcranial alternating current stimulation (tACS) and electroencephalogram (EEG) has been explored in several recent studies. While the analysis of EEG before or after stimulation posits limited technical challenges, the EEG recording during stimulation is heavily affected by the stimulation artifact.

1.1 Matched Phase and Frequency

Computational simulations suggest that the power of endogenous oscillations would increase most if the frequency of tACS matches the targets eigenfrequency (Kutchko and Fröhlich, 2013; Zaehle et al., 2010). This has been supported by evidence from animal studies (Schmidt et al., 2014), and human studies combining tACS with transcranial magnetic stimulation (TMS) (Guerra et al., 2016), or contrasting pre and post resting state power analysis (Zaehle et al., 2010). It has also been suggested that the phase of neuronal populations would be locked to the phase of the tACS signal (Reato et al., 2013). This has been supported by evidence from studies combining tACS with motor output (Brittain et al., 2013), TMS (Raco et al., 2016; Nakazono et al., 2016) or sensory perception (Gundlach et al., 2016).

This suggests that the effect of tACS can result in neurophysiological effects which are phase-and frequency-matched to the stimulation artifact. Such frequency and phase matching between tACS and EEG recordings can render the removal of the artifact difficult or impossible, as the signal might no longer be separatable from the artifact.

1.2 Non-Stationary Amplitude Modulation

An approach to tackle this issue is to assess the time-course of the EEG signal. Consider the assumption that the artifact is stationary and superpositioned on the physiological signal. Then, modulations in the amplitude of the recorded EEG-signal must be caused by changes in the underlying physiology. This would be the case, even if frequency and phase are matched to the stimulation signal. Approaches assuming such stationarity of the stimulation artifact have been used e.g. by Pogosyan et al. (2009).

Yet, detailed analysis of the stimulation artifact provides evidence that the artifact amplitude is actually not stationary. Instead, the amplitude is modulated by heart-beat and respiration (Noury et al., 2016). It has been argued that unregularized spatial filters might be able to remove this amplitude modulation (Neuling et al., 2017). But if only few channels are recorded, the method can fail, as the estimation of the spatial covariance is insufficient, or impossible in the single-channel-case. Consider furthermore that event-related responses like modulation of skin impedance can also affect the scalp conductance at stimulation electrodes. This would introduce event-related amplitude modulation of the stimulation artifact. In that regard, disentangling true signal from the stimulation artifact stays technically challenging.

1.3 Artifact Distortion

Ideally, the stimulation artifict of tACS resembles a sinusoid. Yet, practical experience suggests that the signal is usually distorted to various degrees. Figure 1 shows examples of distortion and saturation in two recordings of tACS-EEG. The gray traces indicate nine invididual periods, while the red trace indicates their average. In figure 1a, note the periodic, yet non-sinusoidal waveform. In figure 1b, note the saturation.

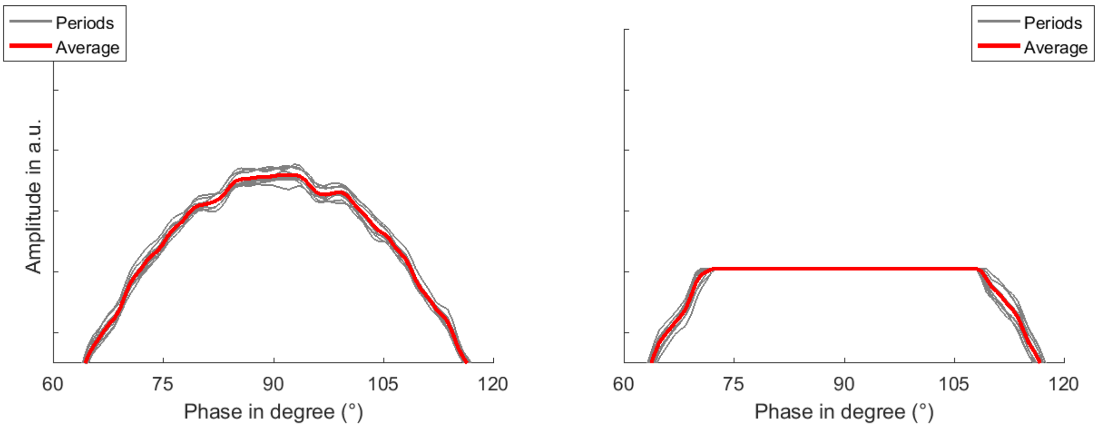

(a) Distortion

(b) Saturation

Figure 1: Examples for loss of sinusoidal fidelity

The temporally and spatially uneven impedance distribution has been suggested as cause of distortion, rendering the resulting waveform periodic, but non-sinusoidal. A major problem is amplifier saturation, i.e. the stimulation artifact exhibiting an amplitude to large for the dynamic range of the amplifier, causing the signal to be cut off and information to be lost. Additionally, non-linearites in the amplifier slew rate can distort the shape even when the signal is close to the saturation threshold. Recently, non-linearities in how stimulators control the applied current has been suggest as further source of modulation (Neuling et al., 2017).

1.4 Computational Demands

Methods based on adaptive template construction and temporal principal component analysis (tPCA) (Niazy et al., 2005) have been explored for removal of non-stationary and misshaped tACS artifacts (Helfrich et al., 2014). Consider that the process of template construction, the estimation of accurate weights for removal by template subtraction and the suqsequent removal of residual artifacts using tPCA is computationally cumbersome. Additionally, it often requires off-line analysis supported by visual inspection. Such a multi-staged template-approach is therefore of limited utility for on-line artifact removal. Furthermore, critical evaluation has suggested that the residual artifact spans several principal components, and a sufficient artifact removal is therefore not possible with tPCA (Noury et al., 2016).

1.5 Rationale

We were interested in development of a computationally fast approach, feasible for online artifact removal. At the same time, the approach was required to account for the dynamical modulation of the artifact amplitude, and the possibility of non-sinusoidal distortion and saturation. Ideally, the approach should allow to estimate physiological signals at the frequency of stimulation, even if physiological oscillations were phase-locked to the stimulation signal.

2 Approach

The main idea is that at any given time point t, the recorded signal $r(t)$ is a linear superposition of a neurophysiological signal $n(t)$, the stimulation artifact $a(t)$ and a white noise term $e(t)$. The task is to recover $n(t)$ by estimating $a(t)$ and $e(t)$ and subtracting from $r(t)$.

$$r(t) = n(t) + a(t) + e(t) \tag{1}$$
$$n(t) = r(t) - a(t) - e(t) \tag{2}$$

2.1 Periodic Estimation

Assume that the tACS artifact were *non-sinusoidal*, but *stationary and periodic*. At the same time, assume that neurophysiological signals n were absent. Then, we could estimate the amplitude of a at any timepoint t by using the recorded signal r any tACS one period length p earlier (3). Subtraction of a delayed version of the signal is also known as comb filter. Please note that for discretely sampled signals, this approach only works if the frequency of the artifact is an integer divisible of the sampling frequency.

$$\hat{a}(t) = r(t - p) \tag{3}$$

2.1.1 Uniform Comb Filter

Consider that white noise term e is still superpositioned on r. Because white noise $\langle e \rangle$ converges asymptotically to zero with increased sample size, an approach to estimate the artifact amplitude could be to average across as many earlier periods as possible (4). Subsequently, this estimate can be used to remove the artifact from r. In real applications, stimulation duration is limited and computational constraints exist. This is reflected by the fact that we have to use a finite number for N.

$$\hat{a}(t) = \sum_{n=1}^{N} \frac{r(t - np)}{N} \tag{4}$$

2.1.2 Superposition of Moving Averages

Please note that averaging across neighbouring periods M (5) has been suggested before and termed superposition of moving averages (SMA) by Kohli and Casson (2015).

$$\hat{a}(t) = \sum_{n-M/2}^{n+M/2} \frac{r(t - np)}{M + 1} \tag{5}$$

Consider that the approach using only past values (4) returns a causal filter. Applied online, a causal filter would be able to remove the artifact without the delay of $(Mp)/2$ necessary for SMA. Furthermore, SMA is well-defined only for even M. This motivates the exploration of causal filters for artifact removal.

2.2 Decay Weighting

More importantly, the artifact amplitude has been described to be non-stationary and dynamically modulated (Noury et al., 2016; Neuling et al., 2017). For real applications, equation (4) can therefore return a biased estimate, depending on whether the integral of this modulation over the time-period $N \times p$ converges to zero. One attempt to tackle with this issue can be the use of a time-dependent weighting function instead of a constant N (6), with the weighting function designed to reduce a possible bias.

$$\hat{a}(t) = \sum_{n=1}^{N} w_n r(t - np) \tag{6}$$

If the dynamics behind the modulation of the artifacts amplitude are known or can be estimated sufficiently, an optimal weighting function can be constructed. Although it has been suggested that there are event-dependent component of the amplitude modulation (e.g. by heartbeat or respiration Noury et al. (2016) or stimulator impedance check Neuling et al. (2017)), the dynamical system governing the event-independent amplitude modulation are usually unknown.

Consider for example a simple comb filter, where we remove the artifact by subtracting the value sampled from any earlier period. Assume now that this values is drawn uniform at random from the last N periods.[1] If the system is fully stationary for the last N periods, performance is virtually identical to the comb filter based on averaging (4). If it is governed by a stochastic process (at least for the last time-points N), e.g. a Wiener process, the precision of the estimate degrades as a function of the delay. This rationale justifies non-uniform weights. In the case of the uniform sampling, we have a single shape parameter N, defining how far back we trust a measurement to have the same precision as earlier samples. By controlling the parameters of alternative weight functions, we might better match the stochastic process governing the amplitude modulation. This might allows us to achieve a better artifact estimation and subsequent removal.

The qualifying criteria for these weighting functions are that the sum of all their weights should be equal to one. This keeps the weighting function in agreement with the average (4), returns an unbiased estimate in the case of full stationarity, and keeps the filter stable. In the following sections, we will discuss three weighting functions assuming non-skewed and unbiased generating processes.

2.2.1 Linear Weighting

One approach is linearization, e.g. using a linear decreasing weighting function. The necessary normalization can easily be implemented by using the triangular number for a given N as normalizing constant k (8). Hence, equation (7) returns weights for earlier periods based on a linear temporal weight decay.

$$w_n = \frac{N - n + 1}{k} \tag{7}$$

with the following normalization

$$k = \sum_{n=1}^{n} n = \frac{N(N+1)}{2} \tag{8}$$

2.2.2 Exponential Weighting

Motivated by the fact that exponentials are an essential building block of signal processing and especially powerful for decay anaylsis, an alternative approach could be an exponential weighting function. The time constant τ of an exponential controls its decay across time. To maintain the shape across different N, we consider it reasonable to normalize n by N. Hence, equation (9) returns weights for earlier periods based on their exponential temporal weight decay.

$$w_n = \frac{1}{k} e^{\tau - \tau(n/N)} \tag{9}$$

with the following normalization

$$k = \sum_{n=1}^{N} e^{\tau - \tau(n/N)} \tag{10}$$

[1]Note, that in the case of full stationarity for the last N periods, its expected performance in the long is expected to be similar to averaging

2.2.3 Gaussian Weighting

Assuming the the precision of the estimate decreaeses over time, a sampling-distribution rationale motivates a Gaussian weighting function. Using a suitable parameterization, and centering on zero, the inverse of the standard deviation $\frac{1}{\sigma^2}$ defines the time constant τ of a Gaussian distribution, which controls its decay. To maintain the shape across different N, we consider it again reasonable to normalize n by N. Hence, equation (11) returns weights for earlier periods based on their exponential temporal weight decay.

$$w_n = \frac{1}{k} f(n/N) \tag{11}$$

with the following generating function and normalization

$$f(x) = \sqrt{\frac{\tau}{2\pi}} e^{-(\tau x^2)/2} \tag{12}$$

$$k = \sum_{n=1}^{N} f(n/N) \tag{13}$$

2.3 Examples

We implemented functions for kernel creation and artifact removal in Matlab 2016b. Additionally, we evaluated them on simulated and real data. Code[2] and data has been published online.

2.3.1 Exemplary Causal Kernels

Examine the following exemplary kernels constructed for a sampling rate of 1KHz, a stimulation frequency of 10 Hz and a memory of 10 2.

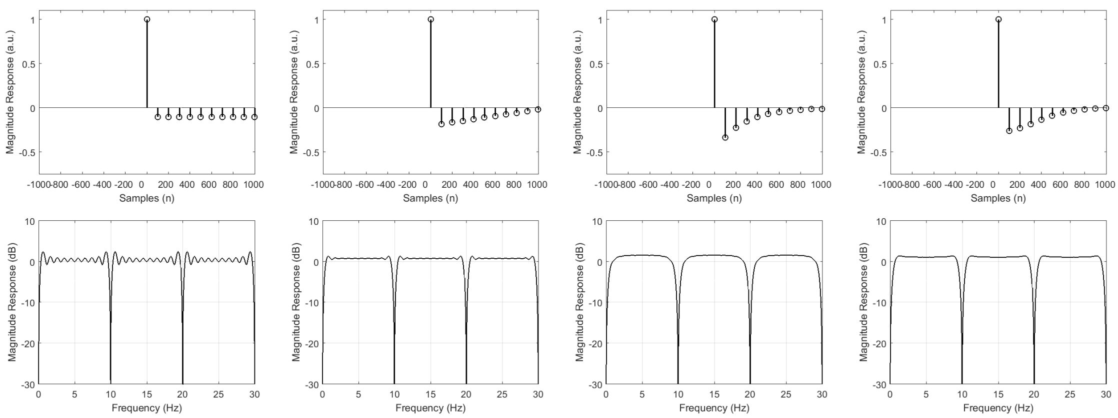

(a) Uniform (b) Linear (c) Exponential $\tau = 4$ (d) Gaussian $\tau = 3$

Figure 2: Exemplary Causal Kernels

As you can see from figure 2, the (numerically calculated) magnitude responses of the four approaches are highly similar. Their key characteristic is the strong supression of the target frequency and its integer multiples. Yet, note the difference in passbands. We find strong ringing in the passband for the uniform 2a and linear kernel 2b, especially compared to the smooth transitions of the exponential 2c or Gaussian kernels 2d.

2.3.2 Exemplary Symmetric Kernels

Examine the following exemplary kernels constructed with parameters identical to the causal kernels, but symmetric on the origin instead 3. Please note that a uniform symmetric would be a SMA-Kernel (5).

[2] `https://github.com/agricolab/ARtACS`

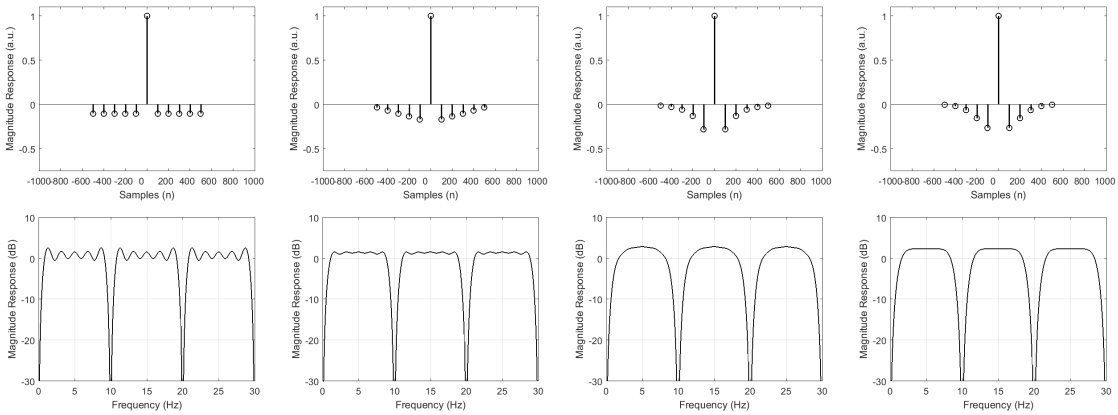

(a) Uniform (b) Linear (c) Exponential $\tau = 4$ (d) Gaussian $\tau = 3$

Figure 3: Exemplary Symmetric Kernels

As you can see from figure 3, symmetric kernels share key characteristic with the causal kernels, especially the strong suppression. But we also find the presence of ringing for the the uniform 3a and linear kernel 3b. Note that the passband range appears to be less narrow for the symmetric compared to the causal filters. Yet the passband response for the Gaussian Kernel exhibits superior flatness 3d.

2.3.3 Exemplary Kernel Tuning

Examine the following exponential kernels constructed with different τ (see figure 4) and N (see figure 5).

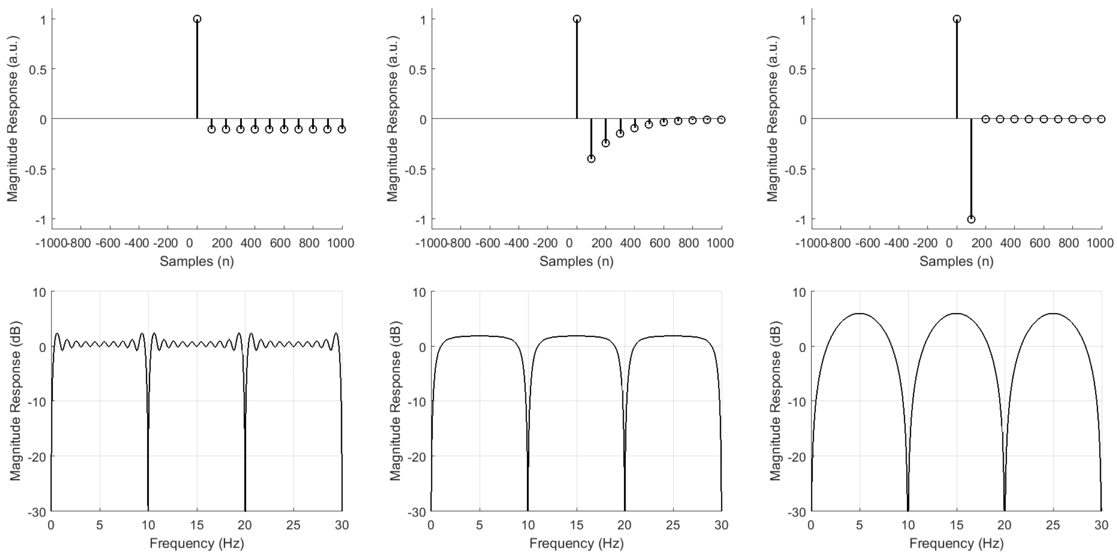

(a) Exponential $\tau = 0$ (b) Exponential $\tau = 5$ (c) Exponential $\tau = 100$

Figure 4: Exemplary τ Tuning with $N = 10$

In the limiting case of $\tau = 0$, the exponential kernel virtually converges with the uniform kernel (see figure 4a). Using a τ equal to the artifacts period length, the exponential kernel almost fully converges with the simple comb filter (see figure 4c). Note that very high tau return an impulse response, and therefore just pass all signals.

In the limiting case of $N = 1$, we acquire the simple comb filter (see figure **??**). By increasing N we achieve a flattening of the pass-band gain (see figure **??**).

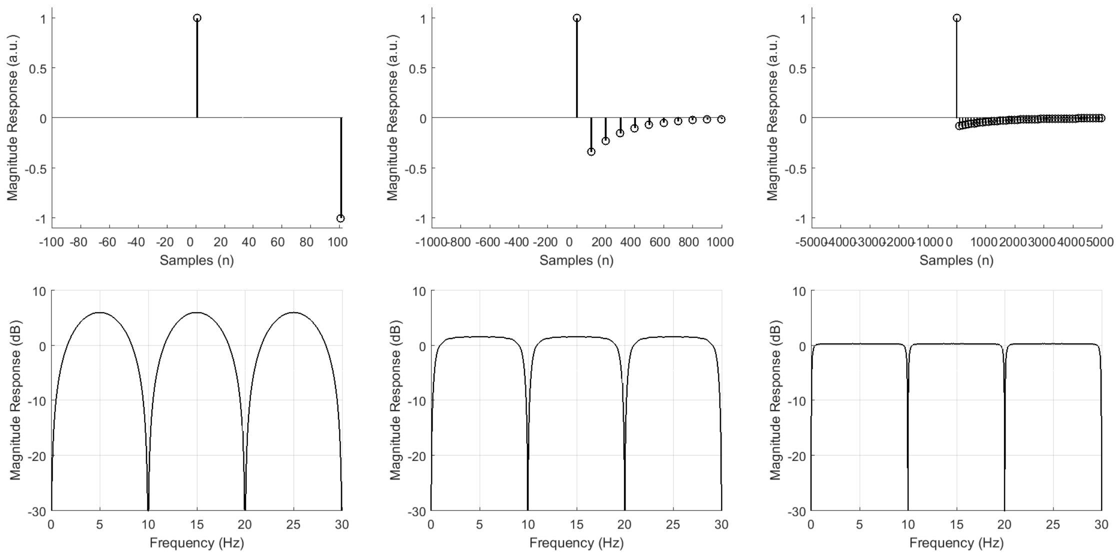

(a) Exponential $N = 1$ (b) Exponential $N = 5$ (c) Exponential $N = 50$

Figure 5: Exemplary N Tuning with $\tau = 3$

3 Evaluation

First, we constructed a kernel based on the respective weighting functions (6) and desired memory, or number of periods N. This kernel was then used to remove the artifact in a recording by convolution. We wanted to evaluate the behavior of the filter in off-line analysis on simulated and real data and decided to use zero-padding for ease of computation.

4 Conclusion

One approach to model such a unknown dynamical system is with a Lévy-process. The key characteristics of such a process is that it is governed by randomness of the change between time-points. The increments are independent from each other, and are sampled from a continuous probability distribution with is stationary for the whole duration of the process. In that framework, the uncertainty of the estimate changes as a function of lag. Consider furthermore that we we only consider

Ornstein-Uhlenbeck-Prozess discrete time AR (1) process

$$a(t+1) = a(t) + \theta(\mu - a(t)) + e(t+1) \tag{14}$$

where $|\theta| < 1$ and μ is the model mean. Note that if the stochastic process is skewed or has a non-zero expectation value, the filter might need to add a constant for debiasing the estimation. If the stochastic process allows for jumps, small N might return a more reliable estimation than large N.

Negative weights This paper only dicusses real filter weights real, but complex weights might be a solution to tackle artifacts with periods that are not integer divisibles of the sampling frequency.

References

Brittain, J.-S., Probert-Smith, P., Aziz, T. Z., and Brown, P. (2013). Tremor suppression by rhythmic transcranial current stimulation. *Current Biology*, 23(5):436–440, DOI: 10.1016/j.cub.2013.01.068.

Guerra, A., Pogosyan, A., Nowak, M., Tan, H., Ferreri, F., Lazzaro, V. D., and Brown, P. (2016). Phase dependency of the human primary motor cortex and cholinergic inhibition cancelation during beta tACS. *Cerebral Cortex*, 26(10):3977–3990, DOI: 10.1093/cercor/bhw245.

Gundlach, C., Müller, M. M., Nierhaus, T., Villringer, A., and Sehm, B. (2016). Phasic modulation of human somatosensory perception by transcranially applied oscillating currents. *Brain Stimulation*, 9(5):712–719, DOI: 10.1016/j.brs.2016.04.014.

Helfrich, R. F., Schneider, T. R., Rach, S., Trautmann-Lengsfeld, S. A., Engel, A. K., and Herrmann, C. S. (2014). Entrainment of brain oscillations by transcranial alternating current stimulation. *Current Biology*, 24(3):333–339, DOI: 10.1016/j.cub.2013.12.041.

Kohli, S. and Casson, A. J. (2015). Removal of transcranial a.c. current stimulation artifact from simultaneous EEG recordings by superposition of moving averages. In *2015 37th Annual International Conference of the IEEE Engineering in Medicine and Biology Society (EMBC)*. IEEE, DOI: 10.1109/embc.2015.7319131.

Kutchko, K. M. and Fröhlich, F. (2013). Emergence of metastable state dynamics in interconnected cortical networks with propagation delays. *PLoS Computational Biology*, 9(10):e1003304, DOI: 10.1371/journal.pcbi.1003304.

Nakazono, H., Ogata, K., Kuroda, T., and Tobimatsu, S. (2016). Phase and frequency-dependent effects of transcranial alternating current stimulation on motor cortical excitability. *PLOS ONE*, 11(9):e0162521, DOI: 10.1371/journal.pone.0162521.

Neuling, T., Ruhnau, P., Weisz, N., Herrmann, C. S., and Demarchi, G. (2017). Faith and oscillations recovered: On analyzing EEG/MEG signals during tACS. *NeuroImage*, 147:960–963, DOI: 10.1016/j.neuroimage.2016.11.022.

Niazy, R., Beckmann, C., Iannetti, G., Brady, J., and Smith, S. (2005). Removal of FMRI environment artifacts from EEG data using optimal basis sets. *NeuroImage*, 28(3):720–737, DOI: 10.1016/j.neuroimage.2005.06.067.

Noury, N., Hipp, J. F., and Siegel, M. (2016). Physiological processes non-linearly affect electrophysiological recordings during transcranial electric stimulation. *NeuroImage*, 140:99–109, DOI: 10.1016/j.neuroimage.2016.03.065.

Pogosyan, A., Gaynor, L. D., Eusebio, A., and Brown, P. (2009). Boosting cortical activity at beta-band frequencies slows movement in humans. *Current Biology*, 19(19):1637–1641, DOI: 10.1016/j.cub.2009.07.074.

Raco, V., Bauer, R., Tharsan, S., and Gharabaghi, A. (2016). Combining TMS and tACS for closed-loop phase-dependent modulation of corticospinal excitability: A feasibility study. *Frontiers in Cellular Neuroscience*, 10, DOI: 10.3389/fncel.2016.00143.

Reato, D., Rahman, A., Bikson, M., and Parra, L. C. (2013). Effects of weak transcranial alternating current stimulation on brain activity—a review of known mechanisms from animal studies. *Frontiers in Human Neuroscience*, 7, DOI: 10.3389/fnhum.2013.00687.

Schmidt, S. L., Iyengar, A. K., Foulser, A. A., Boyle, M. R., and Fröhlich, F. (2014). Endogenous cortical oscillations constrain neuromodulation by weak electric fields. *Brain Stimulation*, 7(6):878–889, DOI: 10.1016/j.brs.2014.07.033.

Zaehle, T., Rach, S., and Herrmann, C. S. (2010). Transcranial alternating current stimulation enhances individual alpha activity in human EEG. *PLoS ONE*, 5(11):e13766, DOI: 10.1371/journal.pone.0013766.